Statistical analysis of historic hydrocarbon production data from Gulf of Mexico oil and gas fields and application to dynamic capacity assessment in CO_2 storage

A. Goudarzi

T. A. Meckel

S. A. Hosseini

R. H. Trevino

Bureau of Economic Geology

Jackson School of Geosciences

The University of Texas at Austin

Correspondence Author: Ali Goudarzi, Bureau of Economic Geology, Jackson School of Geosciences, The University of Texas at Austin, TX 78713-8924, USA.
E-mail: **agoudarzi@utexas.edu**

Keywords: CO_2 storage capacity; Statistical analysis; Gulf of Mexico oil and gas data; Probability of non-exceedance; Dynamic capacity; Decline curve analysis; Constraining boundary conditions

Abstract

Numerical modeling of CO_2 injection and reservoir flow is typically performed to forecast the number of wells, sustainable injection rates, and total storage volume (or mass). A critical determination for CO_2 storage in depleted oil and gas reservoirs is characterization of reservoir compartmentalization which informs boundary conditions in simulating injection scenarios.

Constraining boundary conditions during CO_2 injection into geological formations is a key factor for feasible deployment project. Production history data from 616 wells in 100 oil and gas fields from Gulf of Mexico (GOM) offshore basin can be used to evaluate boundary conditions and total production (oil and gas) and therefor constrain the capacity for potential carbon storage. In general, the combination of decline curve analysis and statistical analysis (to specify constraining boundary conditions) allows the determination of the range of reservoir performance if existing inactive production wells in GOM area of study are used reversibly for CO_2 injection.

To constrain the mass of CO_2 which can be injected, it is useful to consider estimates of cumulative bulk (hydrocarbon + brine) production (CBP), which can be converted to equivalent CO_2 mass considering reservoir conditions. Summary CBP statistics are presented as a probability of non-exceedance (PNE), providing a forecast of likely injection rates and masses for other located CO_2 storage projects with similar geology and boundary conditions in the future. The 50% PNE for Equivalent CO_2 is a novel quantitative approach to investigate the possible injection capacity in CO_2 storage projects. The PNE sensitivity analysis shows that reservoir age, drive mechanism, reservoir trap, and reservoir porosity are the key controlling parameters for productivity and consequently optimum CO_2 storage capacity. Another key finding is the negligible correlation between CBP with reservoir transmissivity and porosity, which implies that other factors than just petrophysical parameters should be studied as constraining factors for CO_2 storage statistical analysis.

1. Introduction

Estimating volumetric CO_2 storage capacity in brine aquifers over large regional areas has been addressed in a variety of ways for decades. The overall focus has been on static capacity calculations, with increased recognition that dynamic factors related to injection need to be

considered (Ganjdanesh and Hosseini, 2018; Meckel et al., 2017). Furthermore, determining the number of wells required to dispose CO_2 emissions by injecting into geological formations is a key factor for feasible project deployment (Mathias et al., 2013a; Ehlig-Economides and Economides, 2010; Cavanagh et al., 2010; Hosa et al., 2011; Gammer et al., 2011). With dynamic assessments, boundary conditions become very influential on results which will be the main focus of this article.

Injection of mega-tons of CO_2 into deep saline aquifers for geologic carbon sequestration (GCS) will create significant pressure perturbations in the subsurface (Birkholzer et al., 2009; Goudarzi et al., 2018; Hosseini and Nicot, 2012; Nicot, 2008; Eiken et al., 2011). The effect of confinement (boundary conditions) on pressure buildup is vital and constraining boundary conditions is paramount. Safety concerns related to these pressure perturbations include 1) seismicity, 2) storage integrity compromise via wells, faults and fractures, and topseal, and 3) impact on underground sources of drinking water due to seepage (Nicol et al., 2011; Oldenburg and Unger, 2003).

The most crucial parameters influencing injectivity are permeability, porosity, formation thickness, areal extent, pressure, temperature, brine salinity and relative permeability (Mathias et al., 2011; 2013b). The values for these parameters in regions with historic and contemporary oil and gas industries are typically available in national and corporate databases (Wilkinson et al., 2011). However, researchers are often limited to using data from the literature, associated with different geological environments (Dria et al., 1993; Bennion and Bachu, 2008; Perrin and Benson, 2010; Pickup et al., 2011; Krevor et al., 2012; Hosseininoosheri et al., 2018).

This research focuses on depleted oil and gas reservoirs in offshore GOM, which have dense data, but the results are considered applicable to adjacent brine reservoirs with similar geology.

This article constrains boundary conditions and potential injection rates and therefor number of wells for future planned CO_2 storage projects in offshore GOM by performing a statistical analysis of production data from 100 oil and gas fields (**Fig. 1**).

The Lower Miocene is the primary historical (1950's to 1980's) hydrocarbon producing zone in offshore Texas and Louisiana and gas (methane) is the dominant historically-produced hydrocarbon. This study utilizes production history data from wells in the study area to evaluate the degree of compartmentalization and anticipated boundary conditions that could be used to inform individual reservoir simulations. Production data statistics for offshore GOM oil and gas fields are used to investigate optimal CO_2 storage reservoir characteristics, including drive mechanism, reservoir age, reservoir trap type, and transmissivity.

The production history and geological data for offshore GOM oil and gas fields were obtained from Seni et al. (1997). The data for 100 GOM fields includes monthly production history data (oil, gas, and water) as well as reservoir petrophysical properties, drive mechanisms, trap types, and reservoir age. The volumes reported in surface standard conditions were converted to volumes at reservoir conditions using calculated oil formation volume factor, water formation volume factor, and gas expansion factor.

Decline curve analysis of historical oil and gas production data from 616 wells from fields of interest are presented and used to determine key production decline parameters using a standard decline rate equation. Those parameters are then used to predict cumulative bulk fluid production for each well, regardless of when the well was shut in. Those fluid volumes at reservoir conditions are then converted to equivalent CO_2 volumes, which are considered as analogs for injectable CO_2 mass at those same (and other similar) sites. This is a simplistic but constrained estimate of dynamic CO_2 storage capability of similar reservoirs. It should be further added that

the amount of dissolved CO_2 in formation brine is assumed to be negligible. This is a reasonable assumption since our focus is mainly on oil and gas reservoirs in GOM but the results can be applied to brine reservoirs as well.

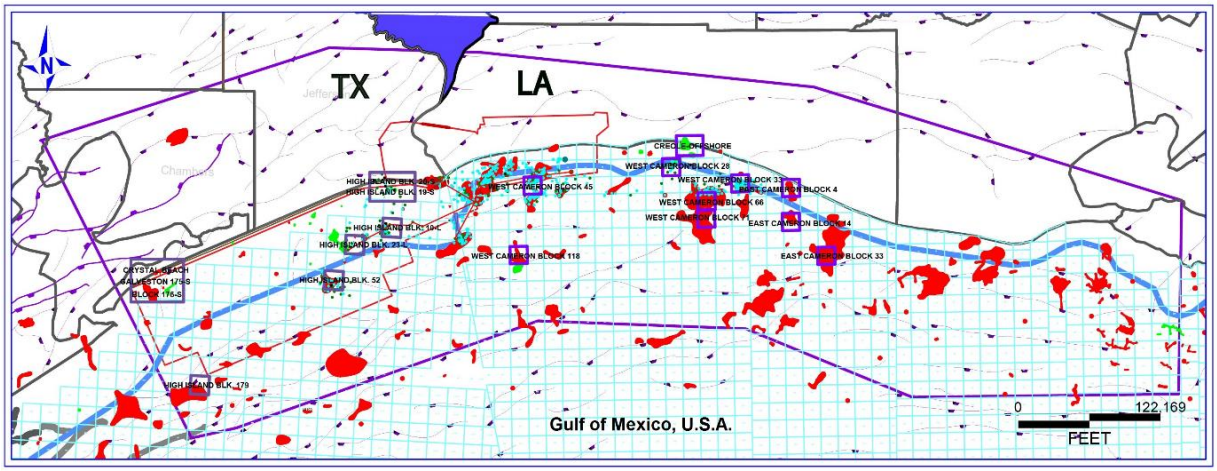

Fig. 1: The geographical location of the offshore GOM CO_2 storage project study area (purple polygon) used for statistical analysis of historic hydrocarbon production. The area of study shows the distribution of the fields of interest. Normal faults (purple curves) can be traced over considerable distances (tens of km) along strike (NW-SE). Oil (green) and gas (red) fields are indicated and offshore blocks are highlighted in cyan.

2. Production Data Decline Analysis

Decline curves are one of the most extensively used forms of data analysis employed in the evaluation of oil and gas fields. Production decline analysis is a traditional means of identifying well production problems and predicting well performance and life based on actual production data. Decline curves are plotted to show a graphical representation of all available production data, and illustrate the temporal decline in produced volumes throughout production. Decline curve analysis uses empirical decline models without knowing reservoir properties and yet proves to be a reliable tool in production forecast. Common models are: a) Exponential decline (constant fractional decline), b) Harmonic decline, and c) Hyperbolic decline. These three models are related through the following relative decline rate equation:

$$\frac{(dq/dt)}{q} = -Dq^b \,, \tag{1}$$

where D and b are empirical constants determined for each well by curve fitting production data. When b = 0, the equation represents an exponential decline model, and when b = 1, it represents a harmonic decline model and for 0 < b < 1, it yields a hyperbolic decline model. The decline rate is a constant with value D (1/Day). If production rate and time data are available, the D-value is the slope of the straight line on a semi-log plot. The D value can then be used to predict production rate at any specific time t and then to calculate cumulative gas production for a specific future time t as shown in **Table 1**. The production behavior and decline curve analysis for two different wells with high and low decline rates are shown in **Fig. 2**. It should be noted that the production history for these two wells were in the range from 1979 to 1984 and decline curve analysis will allow prediction of production for approximately 30 years in this study.

Fig. 3 compares total gas production for four different GOM fields. The blue bar refers to total gas production at the end of actual historic production and the red bar present the total potential gas production after 30 years (had the well continued production instead of being shut in) which is predicted using decline curve analysis. The green date at the top of each blue bar indicates the end of production date which has been reported for that specific well. It is assumed that after that date the well was essentially shut in and or plugged and abandoned. Figure 3a for High Island Block 14-L illustrate that there are some wells (4, 12) which show large differences between the blue and red columns, suggesting a significant amount of unrecovered hydrocarbon, probably due to low oil and gas price at the time. Other wells (1, 15) have been nearly fully depleted and no more hydrocarbon could likely be produced even after 30 years from last production date. Similar observations can be made at the other 3 fields in Figure 3bcd.

Fig. 4 shows the distribution of decline rates for 616 GOM wells. The majority of data fall

below 0.002 which is a good indication of the wells high potential for gas production in the future. The wells with the best decline rates (lowest slope) are located both in Texas and Louisiana in GOM.

The Cumulative Distribution Function (CDF) plot for decline rate (Fig. 4b) is an appropriate way to describe the distribution of the population of decline rates calculated in this study, and indicates that 85% of the data fall below 0.002 1/Day. Similarly, **Fig. 5** shows the distribution of decline coefficients for the same 616 GOM wells. The CDF plot for decline coefficient (Fig. 5b) shows that 80% of decline coefficients are below 10,000 MCF/Day.

The decline curve analysis results in this section are subsequently used to predict the future production performance of existing wells in GOM. It should be emphasized that decline curve analysis is only applied to gas production data which was the main source of hydrocarbon production. Integrating them with the statistical analysis results (to specify constraining boundary conditions) in the next section will determine the range of reservoir performance if those existing inactive production wells are used reversibly for CO_2 injection. Furthermore, the production data analysis will be used to evaluate the degree of compartmentalization and anticipated boundary conditions during storage.

Table. 1: Different decline curve analysis models: Exponential, Hyperbolic, and Harmonic (Gentry, 1972; Benedict, 1981; Ebrahimi, 2010).

Decline Exponent	Type of DCA	Input Data (Oil and Gas Wells)	Production Rate Decline	Total Oil Production
$b = 0$	Exponential	Flow rate vs. Time	$q_t = q_i\, e^{-Dt}$ $q_i = initial\ production\ rate$ $q_t = production\ rate\ at\ time\ t$	$Q_t = (q_i - q_t)/D$
$0 < b < 1$	Hyperbolic	Flow rate vs. Time	$q_t = q_i\,(1 + bDt)^{-1/b}$ $q_i = initial\ production\ rate$ $q_t = production\ rate\ at\ time\ t$	$Q_t = \frac{q_i^b}{(1-b)D}(q_i^{1-b} - q_t^{1-b})$
$b = 1$	Harmonic	Flow rate vs. Time	$q_t = \frac{q_i}{(1 + Dt)}$ $q_i = initial\ production\ rate$ $q_t = production\ rate\ at\ time\ t$	$Q_t = \frac{q_i}{D}[\ln(q_i) - \ln(q_t)]$

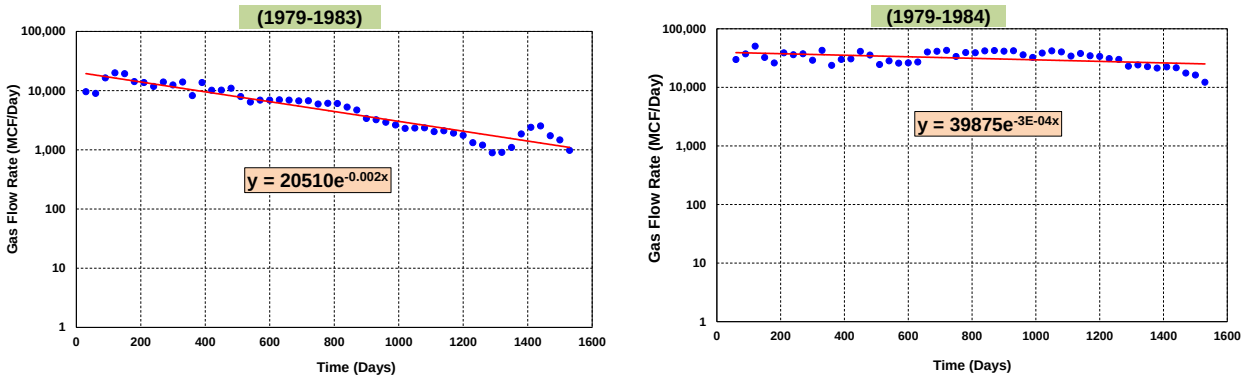

(a) (b)

Fig. 2: The gas production history for two wells: (a) High decline rate of 0.002 with production range of 1979-1983, (b) Low decline rate of 0.0003 with production range of 1979-1984.

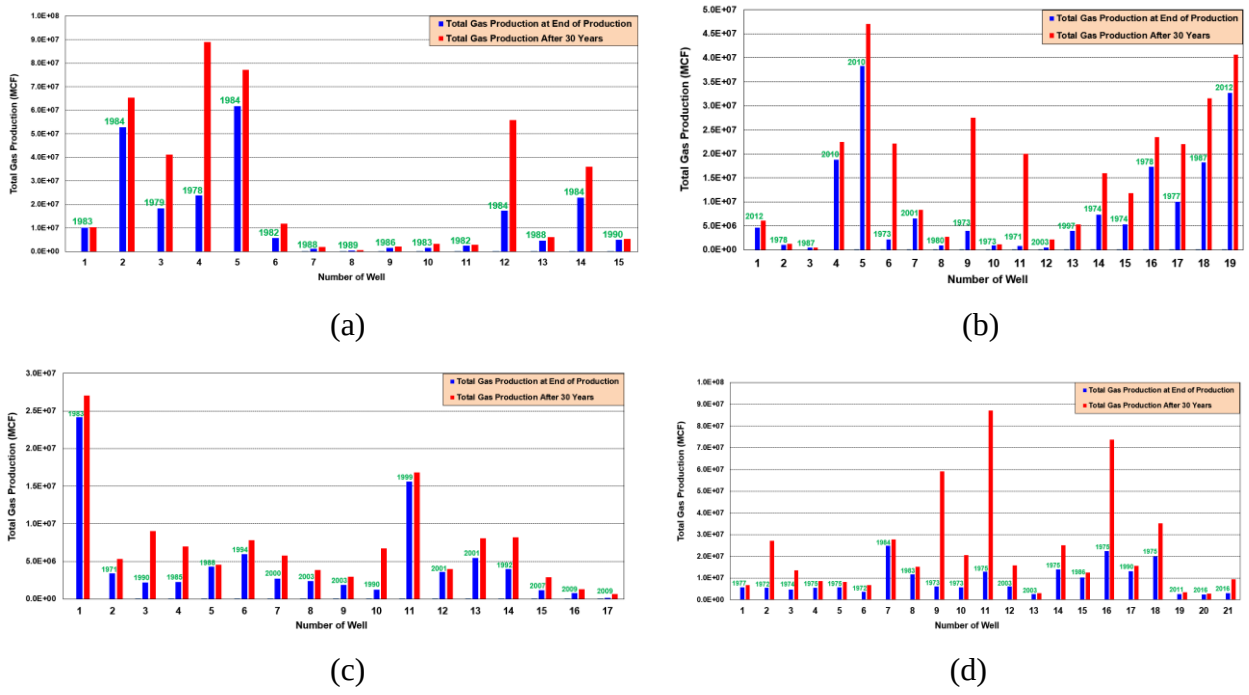

Fig. 3: Comparison of gas production at end of production (blue bars) with forecasted production after 30 years (red bars) for different wells in four different fields: (a) High Island Block 14-L, (b) High Island Block 52-L, (c) East Cameron Block 4, (d) East Cameron Block 14.

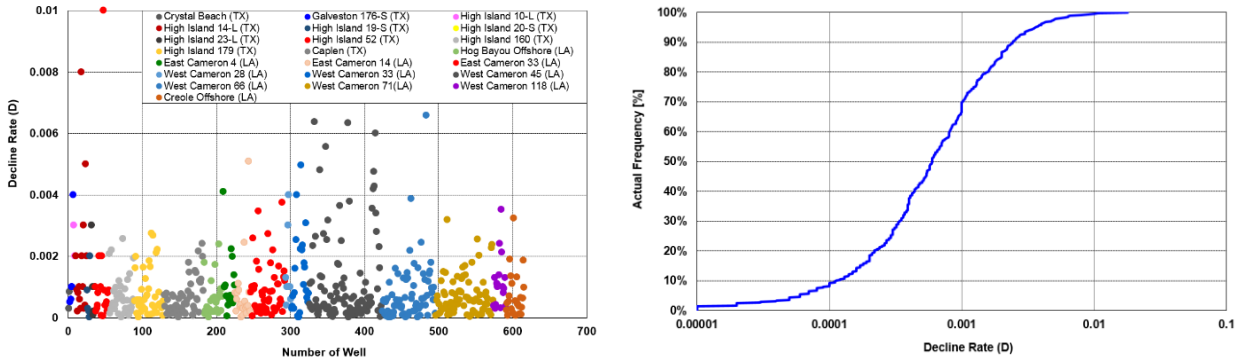

Fig. 4: (a) Distribution of decline rate data for 616 wells in GOM, (b) The CDF plot illustrating the distribution of decline rates in GOM.

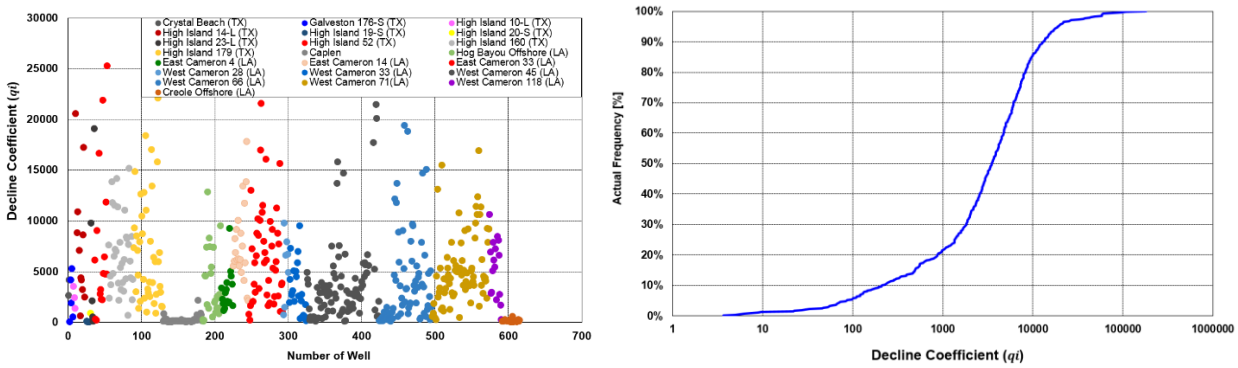

(a) (b)

Fig. 5: (a) Distribution of decline coefficient data for 616 wells in GOM, (b) The CDF plot illustrating the distribution of decline coefficients in GOM.

3. Statistical Analysis of Production Data

To draw insight concerning equivalent mass of CO_2 which can be injected, an estimate of cumulative bulk production (CBP = oil, gas, and water) is considered, found from:

$$CBP = V_o B_o + \frac{V_g}{5.615 E_g} + V_w B_w \,, \tag{2}$$

where CBP denotes cumulative bulk production at reservoir conditions (RC), V_o is total oil production at standard conditions (SC), B_o is oil formation volume factor, V_g is total gas production at standard conditions, E_g is gas expansion factor, V_w is total water production at standard conditions, and B_w is water formation volume factor. The gas expansion factor E_g, is defined as the volume of gas at SC divided by the volume of gas at RC. The oil formation volume factor B_o, is defined as the volume of oil at RC divided by the volume of oil at SC and similar definition holds for water formation volume factor, B_w. Required parameters including initial reservoir pressure, reservoir temperature and etc. for calculating gas expansion factor and volume factors were obtained from Seni et al. (1997).

Note that in order to obtain the average production rate per well, q_{well}, the cumulative bulk production was divided by the number of producing wells in each field as following:

$$q_{well} = \frac{CBP}{N_{well}} . \quad (3)$$

The probability of non-exceedance (PNE) has been calculated using the Weibull plotting position as following (Makkonen, 2006):

$$PNE(q_{well}) = \frac{m}{N+1} , \quad (4)$$

where m is the associated rank number of the value in increasing order and N is total number of observed values for q_{well}.

Another statistical way to visualize data is to plot cumulative distribution (PNE) of production data for 100 fields based on different categories of drive mechanism, reservoir age, reservoir trap, and reservoir transmissivity. **Fig. 6** illustrates how the CBP per well varies in each drive mechanism for arbitrary PNE value of 50%. The mechanisms are waterflood, partial water, pressure depletion, and solution gas. **Fig. 7** shows a similar PNE plot as Fig. 6 but in terms of reservoir age for three categories of Upper Miocene, Middle Miocene, and Lower Miocene. It can be seen from the figure that the categories in order of increasing 50% PNE CBP are Lower Miocene, Middle Miocene, and Upper Miocene. This implies that there is a strong correlation between production rate and reservoir age, with Upper Miocene reservoirs having the best production for 50% PNE (0.87 MMBBL/Year/Well). Upper Miocene reservoirs have seen the least compaction and diagenesis. **Fig. 8** shows how reservoir productivity partitions out for four categories based on reservoir trap designations. The cumulative distribution shows that CBP is not very dependent on reservoir trap type and PNE of 50% have very close values of CBP for four traps with slightly higher values for faulted formations. Therefore, there is a little difference

in statistics for reservoirs with different trap types, suggesting that the flow regime associated with these settings is not dominantly influenced by the type of trap. It should be further realized that PNE of 50% is more representative of the storage process and it is unwise to interpret the higher values of >80% PNE. The comparison of CBP for high and low porosity range indicates that higher porosity in the range of 0.25-0.35 is more favorable with higher CBP as shown in **Fig. 9**.

The plot of CBP vs. reservoir transmissivity data (Transmissivity = reservoir permeability × formation thickness) shows that there is a negligible linear correlation between transmissivity and production data as displayed in **Fig. 10**. Similarly, the calculated average decline rate for 22 reservoirs shows that there is a weak linear correlation between CBP and decline rate as shown in **Fig. 11**. However, the plot of transmissivity (dynamic reservoir parameter) vs. CBP (dynamic capacity parameter) is an innovative regression strategy to classify reservoirs based on different values. Later on, this classification can be used to predict the behavior of a specific reservoir with certain parameters based on previously observed values which illustrates there is room for more research in the future. Overall, PNE and transmissivity plots provide a good basis for using production data in depleted oil and gas reservoirs to gain additional insight concerning constraining boundary conditions during CO_2 injection in future offshore storage projects. To calculate permeability for each reservoir, empirical correlation (porosity vs. permeability) was used which is based on data for Miocene Zone in GOM (Ehrenberg et al., 2008).

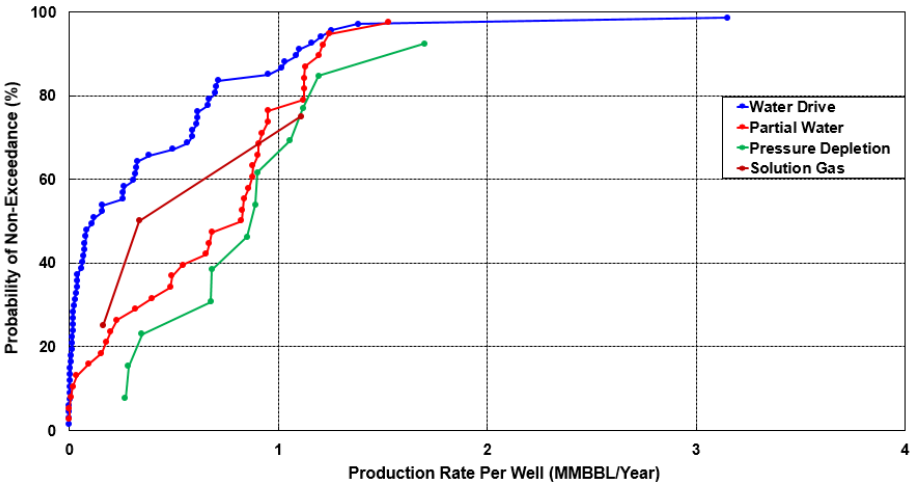

Fig. 6: Cumulative distribution plot (PNE) for CBP per well in terms of drive mechanisms.

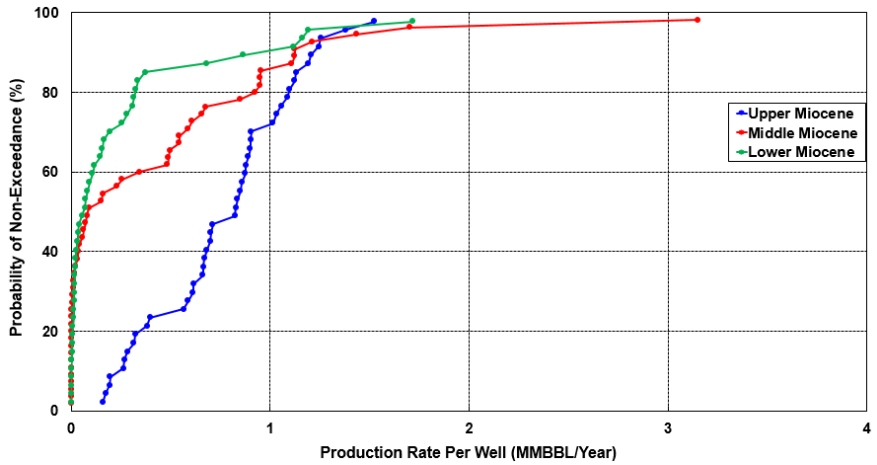

Fig. 7: Cumulative distribution plot (PNE %) for CBP per well in terms of reservoir age.

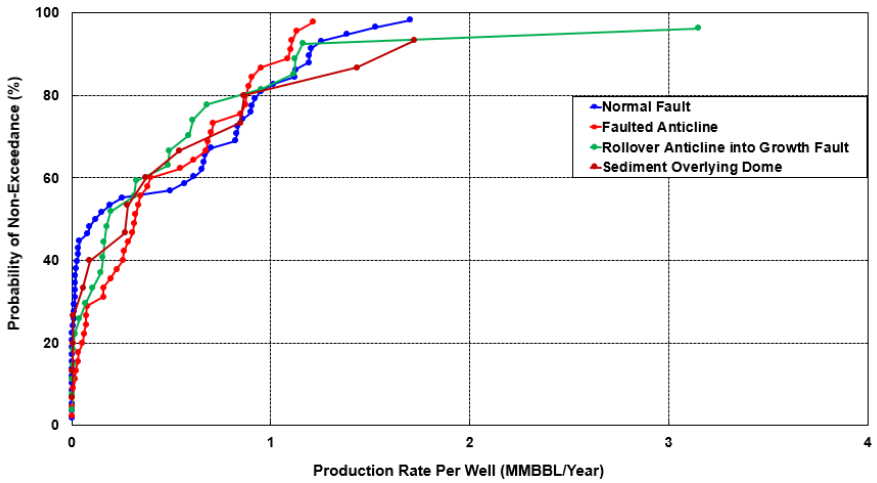

Fig. 8: Cumulative distribution plot (PNE %) for CBP per well in terms of reservoir trap.

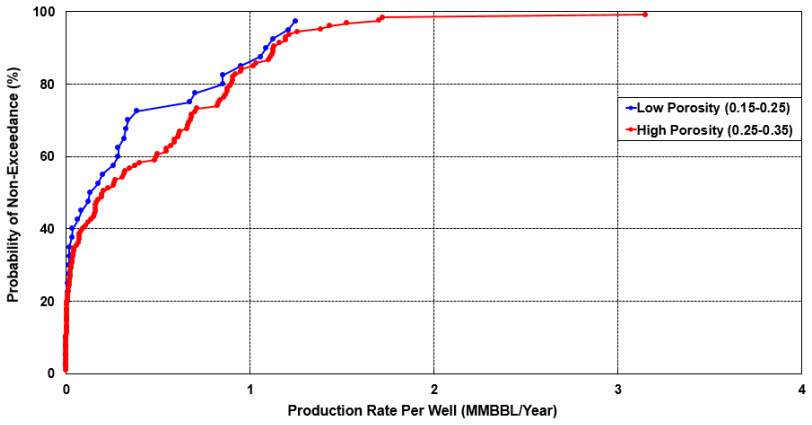

Fig. 9: Cumulative distribution plot (PNE %) for CBP per well in terms of reservoir porosity.

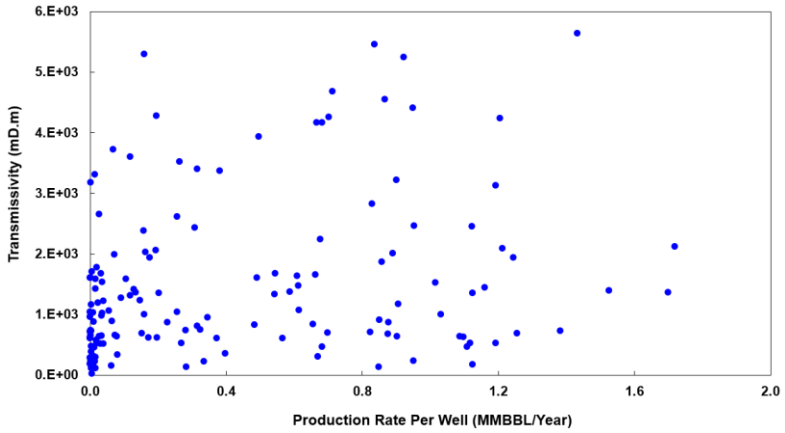

Fig. 10: Plot of production data vs. transmissivities of the reservoirs. Transmissivity is calculated using permeability from Miocene Zone data.

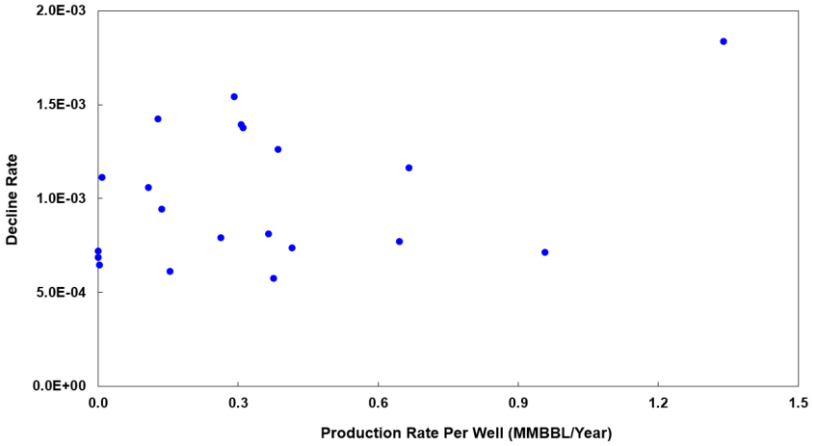

Fig. 11: Plot of production data vs. decline rate of the reservoirs. The average decline rate for each of 22 fields was calculated using individual well decline rates in each reservoir.

4. Discussion of Possible CO_2 Storage Capacity

In the current section, we use oil, gas and water production data from 100 different fields in GOM area of study to calculate equivalent mass of CO_2 which could potentially be stored (storage capacity). This analysis assumes that injected CO_2 would achieve saturations similar to natural hydrocarbon fields, although detailed numerical simulations not undertaken in this study would be required to verify this. The density of CO_2 for each field at different reservoir pressure and temperature conditions was calculated using empirical correlations and the equivalent mass of CO_2 for each reservoir was obtained from:

$$Equivalent\ Mass\ (CO_2) = CBP \times \rho_{CO_2}\ , \tag{5}$$

where ρ_{CO_2} represents CO_2 density at reservoir conditions of T_{res}, P_{res}. **Fig. 12** illustrates how the total of amount CO_2 which can be injected in each historic hydrocarbon field is categorized based on various drive mechanisms. The 50% PNE illustrates that there is probability of injecting 2.14 megatons Equivalent CO_2 in any reservoir classified as Water Drive, 8.81 megatons Equivalent CO_2 in Partial Water, 19.65 megatons Equivalent CO_2 in Pressure Depletion, and 69.63 megatons Equivalent CO_2 in Solution Gas fields. The PNE study illustrates that the amount of Equivalent CO_2 which can be stored are widely distributed from less than one megaton to maximum of 350 megatons. The 50% PNE for Equivalent CO_2 from different characteristics (drive mechanism, reservoir age, and reservoir trap) which is based on statistical analysis of hydrocarbon production data can be a novel quantitative approach to investigate the possible injection capacity in CO_2 storage projects. The reasoning for Partial Water higher Equivalent CO_2 compared to Water Drive is that the PNE study in this article is based on 100 fields in GOM offshore and each of those fields have different petrophysical properties such as depth, thickness, area, porosity, permeability, pressure, temperature, etc. The total storage

capacity for all 100 analyzed fields was about 3300 megatons.

Another important parameter affecting CO_2 capacity quantification is reservoir age. **Fig. 13** shows a similar PNE plot as Fig. 12 but in terms of reservoir age for three categories of Upper Miocene, Middle Miocene, and Lower Miocene. Similar to Fig. 7 for production rates, Fig. 13 illustrates that Upper Miocene reservoirs have the highest 50% PNE values.

Fig. 14 shows how reservoir storage capacity partitions out for four categories based on reservoir trap. Reservoir trap designations include: Normal Fault, Faulted Anticline, Rollover Anticline into Growth Fault, and Sediment overlying Dome. It can be seen that there is little difference between Equivalent CO_2 statistics associated with different reservoir traps. The comparison of Equivalent CO_2 in terms of reservoir porosity indicates favorable conditions can be achieved with high porosity in the range of 0.25-0.35 as shown in **Fig. 15.**

Similar to Fig. 10, the plot of total amount of CO_2 which can be injected vs. reservoir transmissivity data shows that there is a negligible linear correlation between transmissivity and CO_2 injection capacity as shown in **Fig. 16.** It should be noted that formation thickness was obtained from well logs and permeability was calculated using empirical correlations and transmissivity which essentially shows the flow potential and future performance of a reservoir is in fact the product of these two parameters as explained before. Similar to Fig. 11, there is a weak linear correlation between Equivalent CO_2 and decline rate as shown in **Fig. 17**.

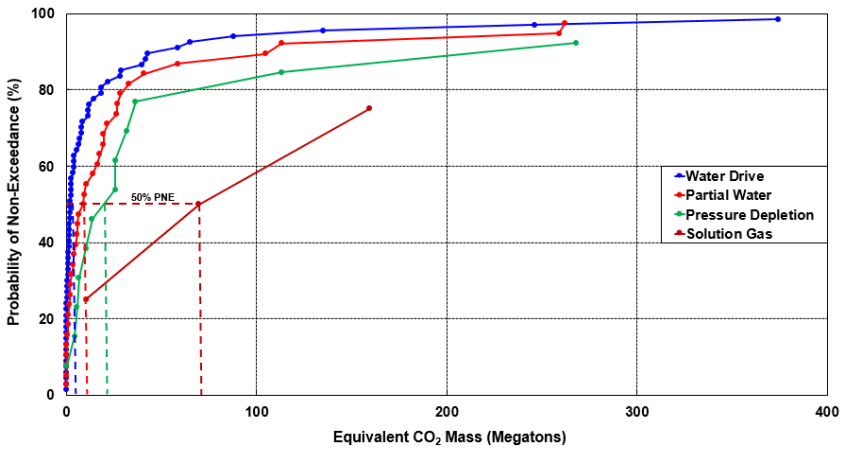

Fig. 12: Cumulative distribution plot (PNE %) for total amount of CO_2 can be injected per each field in terms of drive mechanism.

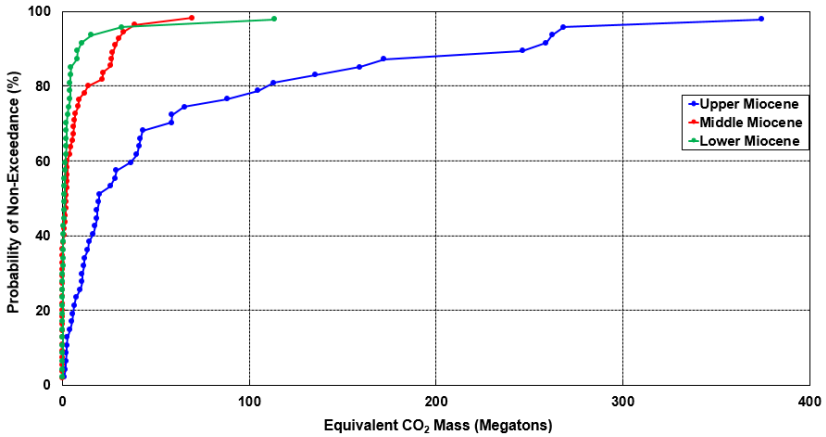

Fig. 13: Cumulative distribution plot (PNE %) for total amount of CO_2 can be injected per each field in terms of reservoir age.

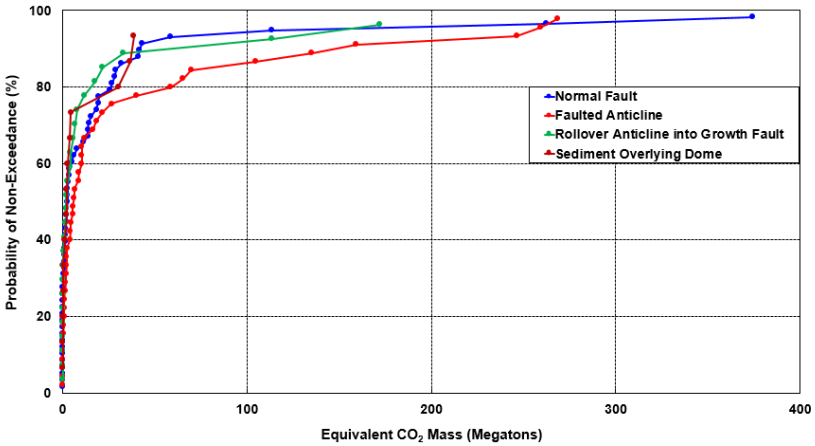

Fig. 14: Cumulative distribution plot (PNE %) for total amount of CO_2 can be injected per each field in terms of reservoir trap.

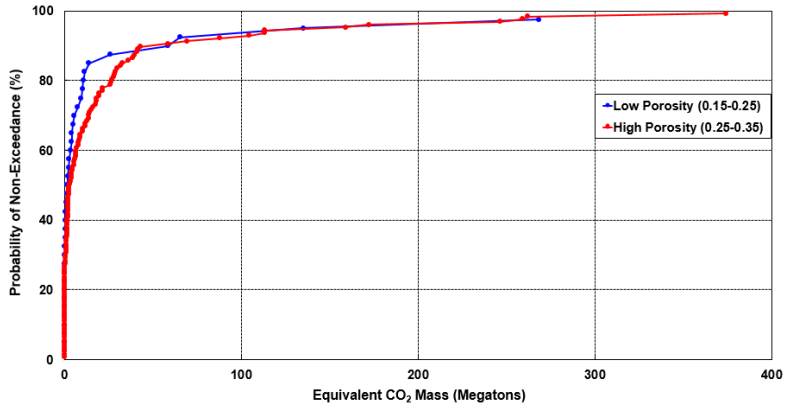

Fig. 15: Cumulative distribution plot (PNE %) for total amount of CO_2 can be injected per each field in terms of reservoir porosity.

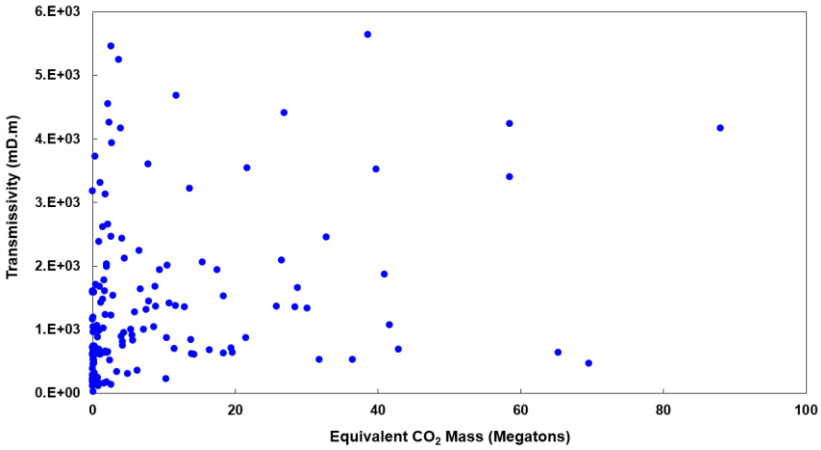

Fig. 16: The plot of total amount of CO_2 can be stored vs. transmissivities of the reservoirs.

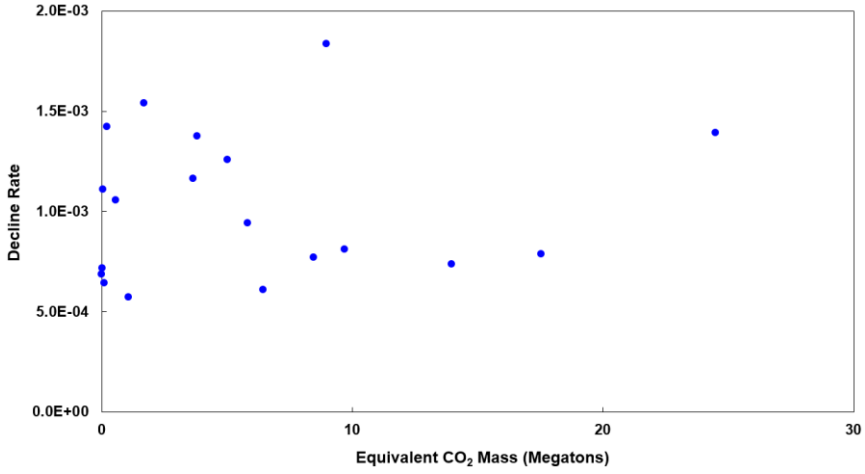

Fig. 17: The plot of total amount of CO_2 can be stored vs. decline rate for 22 fields in GOM.

5. Summary and Conclusions

The objective of this article is to present a statistical investigation of historic hydrocarbon production rates in Gulf of Mexico offshore oil and gas reservoirs, and to consider how those results may be used to forecast likely injection rates for similarly located CO_2 storage projects in the future. Data reported at standard conditions (Seni et al., 1997) are converted to reservoir conditions and integrated into Cumulative Bulk Production (CBP). The CBP is the composite volume of oil, gas, and water at reservoir conditions and can be considered as a proxy for potentially storable CO_2 volumes.

There is a strong correlation between production rate and reservoir age. The 50% PNE CBP values increase consistently from Lower Miocene, through Middle Miocene, to Upper Miocene age stratigraphy. A statistical sensitivity study indicates that reservoir age, drive mechanism, and reservoir porosity are the crucial controlling parameters on CBP; however, reservoir trap has small impact on CBP. A negligible correlation is found between CBP and reservoir transmissivity and decline rate.

The combination of decline curve analysis and statistical analysis (to specify constraining boundary conditions) allows the determination of the range of reservoir performance if existing inactive production wells in GOM area of study are used reversibly for CO_2 injection. Furthermore, the production data analysis is used to evaluate the degree of compartmentalization and anticipated boundary conditions during storage.

The 50% PNE for Equivalent CO_2 is a novel quantitative approach to investigate the possible injection capacity in CO_2 storage projects. The important point is that the PNE study in this article is based on 100 fields in GOM offshore and each of those fields have different petrophysical properties such as depth, thickness, area, porosity, permeability, etc. For example,

the 50% PNE for Equivalent CO_2 in terms of drive mechanism illustrates that there is 50% probability of injecting 2.14 Megatons Equivalent CO_2 in any individual Water Drive reservoir, 8.81 Megatons Equivalent CO_2 in any Partial Water Drive reservoir, 19.65 Megatons Equivalent CO_2 in any Pressure Depletion Drive reservoir, and 69.63 Megatons Equivalent CO_2 in any Solution Gas field. Although the results of this study are useful to indicate solution gas drive and gas reservoirs are the most promising candidates for CO_2 storage, more studies are required to confirm the finding presented in this paper.

Acknowledgments

This work was conducted with the financial support of the DOE-NETL Offshore Storage Project (DE-FE0026083) at the Gulf Coast Carbon Center. Publication authorized by the director of Bureau of Economic Geology at The University of Texas at Austin.

References

Benedict, J., 1981. CO_2 The Mathematics of Decline Curves. Paper SPE 10537, Society of Petroleum Engineers.

Bennion, D. B. and Bachu, S., 2010. Drainage and imbibition CO_2/brine relative permeability curves at reservoir conditions for carbonate formations. Paper SPE 134028, presented at the SPE Annual Technical Conference and Exhibition, Florence, Italy, September, 19-22.

Birkholzer, J. T., Zhou, Q., and Tsang, C. F., 2009. Large-scale impact of CO_2 storage in deep saline aquifers: a sensitivity study on the pressure response in stratified systems. *International Journal of Greenhouse Gas Control*, 3: 181-194.

Cavanagh, A. J., Haszeldine, R. S., Blunt, M. J., 2010. Open or closed? A discussion of the mistaken assumptions in the Economides pressure analysis of carbon sequestration. *Journal*

of Petroleum Science and Engineering, 74(1): 107–110.

Dria, D. E., Pope, G. A., and Sepehrnoori, K., 1993. Three-Phase Gas/Oil/Brine Relative Permeabilities Measured Under CO_2 Flooding Conditions. *SPE Reservoir Engineering Journal*, 8(2): 143-150.

Ebrahimi, M., 2010. Enhanced Estimation of Reservoir Parameters Using Decline Curve Analysis. Paper SPE 133432, presented at the Trinidad and Tobago Energy Resources Conference, Port of Spain, Trinidad, June, 27-30.

Ehlig-Economides, C. and Economides, M. J., 2010. Sequestering carbon dioxide in a closed underground volume. *Journal of Petroleum Science and Engineering*, 70(1): 123–130.

Ehrenberg, S. N., Nadeau, P. H., and Steen, Q., 2008. A megascale view of reservoir quality in producing sandstones from the offshore Gulf of Mexico. *AAPPG Bulletin Journal*, 92: 145–164.

Eiken, O., Ringrose, P., Hermanrud, C., Nazarian, B., Torp, T. A., and Hoier, L., 2011. Lessons Learned from 14 years of CCS Operations: Sleipner, In Salah and Snohvit. *Energy Procedia*, 4: 5541-5548.

Gammer, D., Green, A., Holloway, S., and Smith, G., 2011. The Energy Technologies Institute's UK CO_2 Storage Appraisal Project (UKSAP).

Ganjdanesh, R., and Hosseini, S. A., 2018. Development of an analytical simulation tool for storage capacity estimation of saline aquifers. *International Journal of Greenhouse Gas Control*, 74: 142-154.

Gentry, R. W., 1972. Decline-Curve Analysis. *Journal of Petroleum Technology*, 24(1): 38-41.

Goudarzi, A., Hosseini, S. A., Sava, D., and Nicot, J. P., 2018. Simulation and 4D seismic studies of pressure management and CO_2 plume control by means of brine extraction and

monitoring at the Devine Test Site, South Texas, USA. *Journal of Greenhouse Gases: Science and Technology*, 8:185-204.

Hosa, A., Esentia, M., Stewart, J., and Haszeldine, S., 2011. Injection of CO_2 into saline formations: benchmarking worldwide projects. *Chemical Engineering Research and Design*, 89(9): 1855–1864.

Hosseini, S. A. and Nicot, J. -P., 2012. Numerical modeling of a multiphase water-oil-CO_2 system using a water-CO_2 system: Application to the far field of a U.S. Gulf Coast reservoir. *International Journal of Greenhouse Gas Control*, 10: 88-99.

Hosseininoosheri, P., Hosseini, S.A., Nuñez-López, V., and Lake, L.W., 2018. Evolution of CO_2 Utilization Ratio and CO_2 Storage under Different EOR Operating Strategies: A Case Study on SACROC Unit (Permian Basin). Paper SPE 190038, presented at SPE Western Regional Meeting, California, USA, April, 22-27.

Kreover, S. C. M., Pini, R., Zuo, L, and Benson, S. M., 2012. Relative permeability and trapping of CO_2 and water in sandstone rocks at reservoir conditions. *Water Resources Research*, 48(2): 1-16.

Makkonen, L., 2006. Plotting positions in extreme value analysis. *Journal of Applied Meteorology and Climatology*, 45(2): 334–340.

Mathias, S. A., de Miguel, G. J. G. M., Thatcher, K. E., and Zimmerman, R. W., 2011. Pressure buildup during CO_2 injection into a closed brine aquifer. *Transport in Porous Media*, 89(3): 383–397.

Mathias, S. A., Gluyas, J. G., Mackay, E. J., and Goldthorpe, W. H., 2013a. A statistical analysis of well production rates from UK oil and gas fields – Implications for carbon capture and storage. *International Journal of Greenhouse Gas Control*, 19: 510-518.

Mathias, S. A., Gluyas, J. G., González Martínez de Miguel, G. J., Bryant, S. L., and Wilson, D., 2013b. On relative permeability data uncertainty and CO_2 injectivity estimation for brine aquifers. *International Journal of Greenhouse Gas Control*, 12: 200–212.

Meckel, T. A., Trevino, R., and Hovorka, S. D., 2017. Offshore CO_2 Storage Resource Assessment of the Northern Gulf of Mexico. *Energy Procedia*, 114: 4728-4734.

Nicol, A., Carne, R., Gerstenberger, M., and Christophersen, A., 2011. Induced Seismicity and its Implications for CO_2 Storage Risk. *Energy Procedia*, 4: 3699-3706.

Nicot, J. -P., 2008. Evaluation of large-scale CO_2 storage on freshwater sections of aquifers: an example from the Texas Gulf Coast Basin. *International Journal of Greenhouse Gas Control*, 2(4): 582-593.

Oldenburg, C. M. and Unger, A. J., 2003. On Leakage and Seepage from Geologic Carbon Sequestration Sites: Unsaturated Zone Attenuation. Vadose Zone Journal, 2: 287–296.

Perrin, J. -C. and Benson, S. M., 2010. An experimental study on the influence of sub-core scale heterogeneities on CO_2 distribution in reservoir rocks. *Transport in Porous Media*, 82(1): 93–109.

Pickup, G. E., Jin, M., Olden, P., Mackay, E. J., and Sohrabi, M. 2011. A Sensitivity Study on CO_2 Storage in Saline Aquifers. Paper SPE 143054, presented at the SPE EUROPEC/EAGE Annual Conference, Vienna, Austria, May, 23-26.

Seni, S. J., Hentz, T. F., Kaiser, W. R., and Wermund, Jr. E. G. 1997. Atlas of Northern Gulf of Mexico Gas and Oil Reservoirs: Miocene and Older Reservoirs, v. 1: Austin, Texas, The University of Texas at Austin, Bureau of Economic Geology, 199 p.

Wilkinson, M., Haszeldine, R. S., Hosa, A., Stewart, R. J., Holloway, S., Bentham, M., Smith, K., Swarbrick, R., Jenkins, S., Gluyas, J., Mackay, E., Smith, G., Daniels, S., and Raistrick,

M., 2011. Defining simple and comprehensive assessment units for CO_2 storage in saline formations beneath the UK North Sea and continental shelf. Energy Procedia 4, 4865–4872.